Rev.Adv.Mater.Sci. 18(2008) 744-749

ON THE STRUCTURE AND STABILITY OF ZrNi SYSTEM

A. Al-Hajry

Department of Physics, College of Science, King Khalid University, Abha, P.O.Box 9003, Saudi Arabia

Received: March 29, 2008

Abstract. The atomic structure of amorphous phases in ZrNi system prepared by fast quenching (FQ) and mechanical alloying (MA) are compared on an atomic scale using the reduced radial distribution function *G*(*r*), then investigated by thermal methods. The amorphous structure is characterized by X-ray diffraction (XRD). Differential scanning calorimetry (DSC), was used to investigate the crystallization kinetics. It is found that both FQ and MA ZrNi specimens have similar crystallization kinetics under non-isothermal conditions. However, the FQ ZrNi is much more stable compared with its MA counterpart.

1. INTRODUCTION

There is a considerable interest in the amorphous alloys of early-late transition metals, due to their basic physical properties and potential technological applications. To be used in specific technological applications, such materials should have stable structures both with time and temperature of the required application. ZrNi system is one of the many early-late transition metal alloys that that has been successfully obtained by MA [1-3]. The present ZrNi specimen has been studied earlier [4] in regards to its amorphous structure. Two specimens of the same atomic concentrations prepared by FQ and MA techniques were compared by the reduced radial distribution function *G*(*r*). It turns out that although the two amorphous specimens were synthesized by two different techniques; the final products are quite similar on an atomic scale. The objective of this work is to investigate the crystallization kinetics of two amorphous states of the ZrNi system prepared by FQ and MA techniques. The *G*(*r*) calculation makes any subsequent thermal studies more useful since the atomic structures on an atomic scale (the short range order SRO) of amorphous phases studied are determined, in advance. Therefore, two amorphous $Zr_{65}Ni_{35}$ specimens prepared by FQ and MA are structurally compared using the *G*(*r*) function. If both are identical on an atomic scale, then they are good candidates for the investigation by thermal methods. The crystallization kinetics of these two specimens are investigated under non-isothermal conditions, to assess whether they have the same thermal behaviour.

2. EXPERIMENTAL METHODS

$Zr_{65}Ni_{35}$ (at. %) alloy ingots, were arc-melted of pure Zr and Ni wires with purity of better than 99.9, which were then fast quenched (FQ) at ~ 4500 rpm, to produce metallic glass ribbons (25 μm thick, and 2 mm wide) in an atmosphere of purified argon. Another specimen of the same composition was prepared by mechanical alloying (MA), in order to be investigated and compared with its counterpart ($Zr_{65}Ni_{35}$ prepared by FQ). Parent powders of the Zr and Ni elements were mixed and mechanically alloyed in a hardened steel vial of a Spex mixer (model 8001) using 4 grams and two 1/2” steel

Corresponding author: A. Al-Hajry, e-mail: ahajry@kku.edu.sa

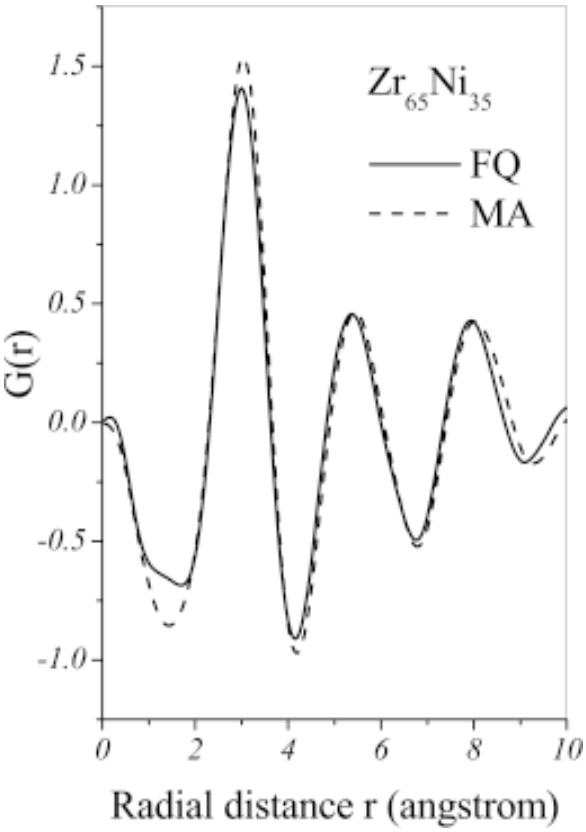

Fig. 1. The reduced radial distribution function $G(r)$ of both amorphous phases of the FQ and MA $Zr_{65}Ni_{35}$ specimens.

balls. The process was carried out under an argon atmosphere to prevent oxidation. The balls to powder ratio was 4.15:1. A full amorphous $Zr_{65}Ni_{35}$ phase was obtained after 5 h of MA time. The structure of the specimens throughout this study was determined by an X-ray diffractometer of vertical goniometer (Shimadzu XRD-6000) equipped with a curved crystal graphite monochromator (MoK_{α}=0.7093 Å). The molybdenum target is used to get a wide range covered by the scattering vector Q (where $Q=4\pi\sin(\theta)/\lambda$Å^{-1}) in order to resolve the atomic structure on an atomic scale for the amorphous ZrNi. The thermal stability and kinetics of the specimens were studied using a Shimadzu DSC-50 thermal analyser. The specimens of about 20 mg are heated in platinum pans in an atmosphere of dry nitrogen at a flow rate of 40 ml/min. A reference powder of Al_2O_3 was used. The temperatures and energies of the DSC analyser were calibrated using known temperatures and energies of a standard, leading to an accuracy of 0.1K and 0.02 mW for temperature, and energy respectively. Non-isothermal DSC scans were performed in a range of 10 up to 35 K/min, where each scan is performed from room temperature up to 700 °C. A short programme (on MATLAB) was written to derive the crystallized volume fraction c according to the procedure explained in a previous work [5]. The activation energy for crystallization E_a was derived using the best fit for the results by the least squares method, where the arithmetic mean and standard deviation for the activation energies are evaluated.

3. RESULTS AND DISCUSSION

3.1. X-ray diffraction

The X-ray intensity data collected by the molybdenum target were corrected and normalized to get the appropriate total structure factor $S(Q)$ as discussed elsewhere [4], then Fourier transformed to get the reduced radial distribution function $G(r)$ which can be written as

$$G(r)=4\pi\{\rho(r)-\rho_0\}\int_0^{Q_{max}} Q\{S(Q)-1\}\sin(Qr)dQ, \quad (1)$$

where r is the radial distance from a reference atom, $\rho(r)$ and ρ_0 are the atomic density at a radial distance r from a reference atom, the average atomic density of the amorphous structure of the specimen respectively, Q_{max} is the maximum measured scattering vector Q. An example of the $G(r)$ results for the FQ and MA $Zr_{65}Ni_{35}$ is shown Fig. 1. The derived radial distances of the nearest neighbouring atoms to a reference atom in the amorphous phase; r_1, r_2, and r_3 are 3.05, 5.53, and 8.13 Å respectively, for the FQ $Zr_{65}Ni_{35}$. These correspond to 3.03, 5.50, and 8.10 Å for the MA $Zr_{65}Ni_{35}$ specimen. These values for the radial distances are in excellent agreement with the weighted averages of the Goldschmit radii $<r_G>$ for this alloy system [4,7]. The $<r_G>$ value calculated for the first peak in the $G(r)$ function is expected to be at 3.00 Å for $Zr_{65}Ni_{35}$ which is very close to 3.05 Å (for the FQ specimen) or 3.03 Å (for the MA specimen) obtained experimentally.

This confirms that the FQ and the MA $Zr_{65}Ni_{35}$ specimens investigated here are quite similar on an atomic scale. As such, these specimens can be investigated and compared by thermal methods more realistically, since any structural differences on an atomic scale are almost eliminated.

Table 1. Some thermal parameters derived for both the FQ and MA $Zr_{65}Ni_{35}$ specimens.

$Zr_{65}Ni_{35}$ Alloy	1st peak*			2nd peak*			3rd peak*		
	T_p (K)	T_c (K)	E_a (kJ/mol)	T_p (K)	T_c (K)	E_a (kJ/mol)	T_p (K)	T_c (K)	E_a (kJ/mol)
FQ	678.4	665.4	366.7	711.2	692.2	205.9	734.3	727.6	285.1
MA	592.1	559.2	126.0	735.5	657.2	146.6	-	-	-

*At 20 K/min, and E_a is calculated here using Kissinger's method.

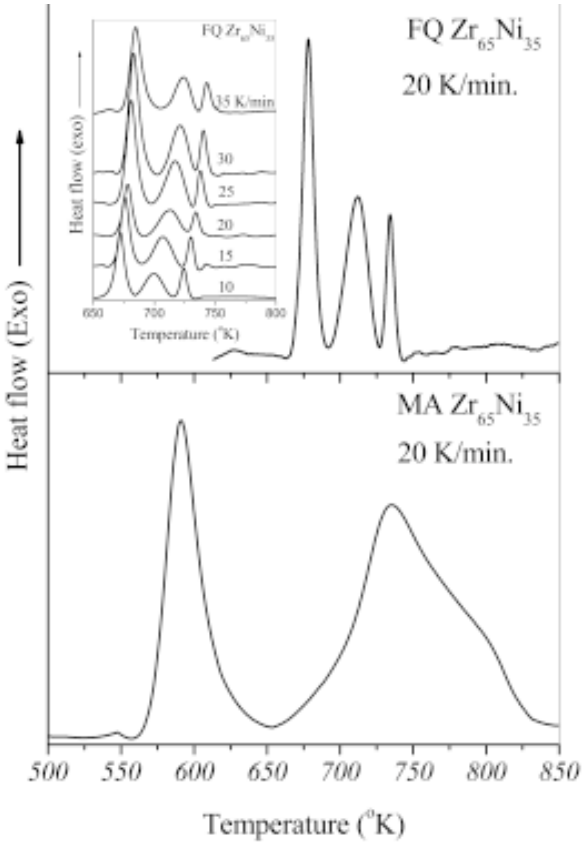

Fig. 2. DSC traces of the FQ and MA $Zr_{65}Ni_{35}$ at a heating rate of 20 K/min. In the inset a full DSC traces for the FQ $Zr_{65}Ni_{35}$ at different heating rates (10 – 35 K/min) are displayed.

3.2. DSC measurements

In order to understand the structural evolution under heating, non-isothermal DCS scans were performed**.** Continuous heat scans have been performed for the specimens at different heating rates ranging from 10 up to 35 K/min, in order to derive some crystallization kinetic parameters for both FQ and MA $Zr_{65}Ni_{35}$ specimens. Fig. 2 shows DSC scans for both FQ and MA $Zr_{65}Ni_{35}$. Also shown in the same figure (as an inset) the DSC scans for the FQ $Zr_{65}Ni_{35}$ at different heating rates (10 – 35 K/min). For the FQ $Zr_{65}Ni_{35}$ specimen, three successive sharp crystallization peaks at well defined temperatures, can be observed. At a heating rate of 20 K/min, these three crystallization peaks are observed at 678.4, 711.2, and 734.3K. This indicates that the crystallization process of the FQ ZrNi takes place in three stages. On the other hand, the MA $Zr_{65}Ni_{35}$ specimen has two crystallization peaks, indicating a double crystallization process. However, the second peak is very broad and it could be composed of two peaks that could not be resolved in the preset experiment. The first peak is sharp at 592.5K and the broad one is at ~ 735K. No distinct glass transition, in the DSC curves for either the FQ, nor for the MA ZrNi has been observed. Such a behaviour has also been reported by other authors [7,8]. The onset crystallization peak for the MA (treated for 5 h) is ~ 570K. This is much smaller than that reported for the $Zr_{64}Ni_{36}$ MA (treated for 60 h) which is reported to be 760K [8]. This difference in the onset crystallization temperature T_c of two specimens mechanical alloyed at two different conditions could reflect the easiness of obtaining the amorphous phase in the present work, compared to the long milling time used to produce the $Zr_{64}Ni_{36}$ specimen [8]. In fact it has been found [4] that the MA alloying process of ZrNi system exhibits what is called a cyclic amorphization property in which multi amorphous states can be achieved. The first amorphous phase obtained by MA process could be missed easily in favour of other crystalline phases, leading to prolonged MA times to find another chance for obtaining another amorphous phase. This has been found by other authors in similar early-late transition alloys (e.g. [see 9]). Therefore, the low T_c obtained for the MA-treated specimen in the present work reflects the

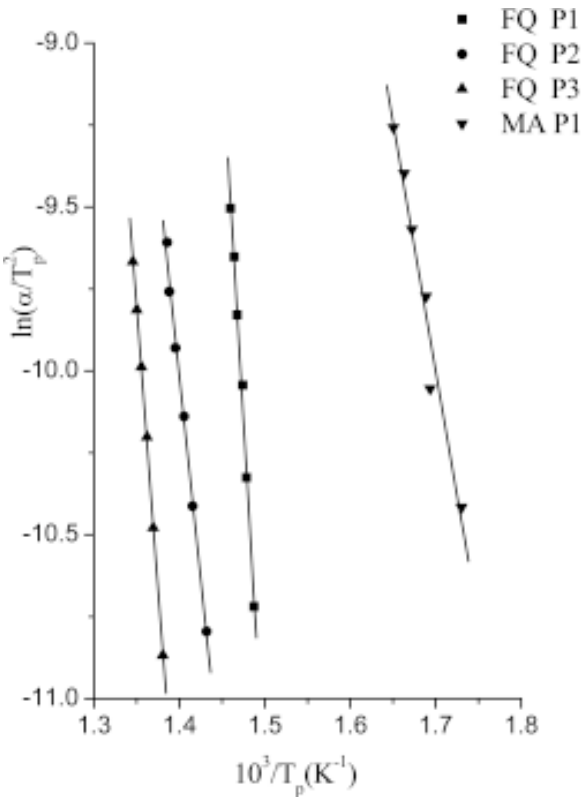

Fig. 3. Kissinger's plots for FQ and MA $Zr_{65}Ni_{35}$ specimens. There are three crystallization peaks for the FQ $Zr_{65}Ni_{35}$ (P_1, P_2, and P_3) considered while only the main peak (P_1) for the MA $Zr_{65}Ni_{35}$ is shown here.

easiness of obtaining specific amorphous phase at a very early stage of MA time, and characterize that specific early amorphous state. According to the Kissinger model [10], the crystallization peak temperature T_p in a DSC scan depends on the heating rate a as follows

$$\ln\left(\frac{\alpha}{T_p^2}\right) = const - \left(\frac{E_a}{RT_p}\right), \qquad (2)$$

where T_p is the peak crystallization temperature, R is the gas constant, E_a is the activation energy for crystallization. A plot of $\ln(\alpha/T_p^2)$ as a function of $1/T_p$ should give a straight line with a slope of E_a/R. As seen in Fig. 2 there are three crystallization peaks representing the crystallization events clearly observed for the FQ $Zr_{65}Ni_{35}$ specimen. The activation energy E_a is calculated for these three peaks according to Eq. (2) and the result is shown in Fig. 3. E_a for these peaks are 366.7, 205.9, and 285.1 kJ/mole respectively. On the other hand, for the MA specimen, the calculated activation energy E_a using the first peak is 126 kJ/mole, and 146.6 kJ/mole for the second peak. These values are much

Table 2. The Avrami exponent *n* values for both the FQ and MA $Zr_{65}Ni_{35}$ specimens obtained under non-isothermal conditions.

	Avrami exponent *n*	
Temperature (K)	FQ $Zr_{65}Ni_{35}$	MA $Zr_{65}Ni_{35}$
678	3.8 ± 0.3	3.6 ± 0.4
680	3.1 ± 0.4	3.1 ± 0.4
683	2.5 ± 0.3	2.4 ± 0.4
685	2.3 ± 0.2	2.2 ± 0.3

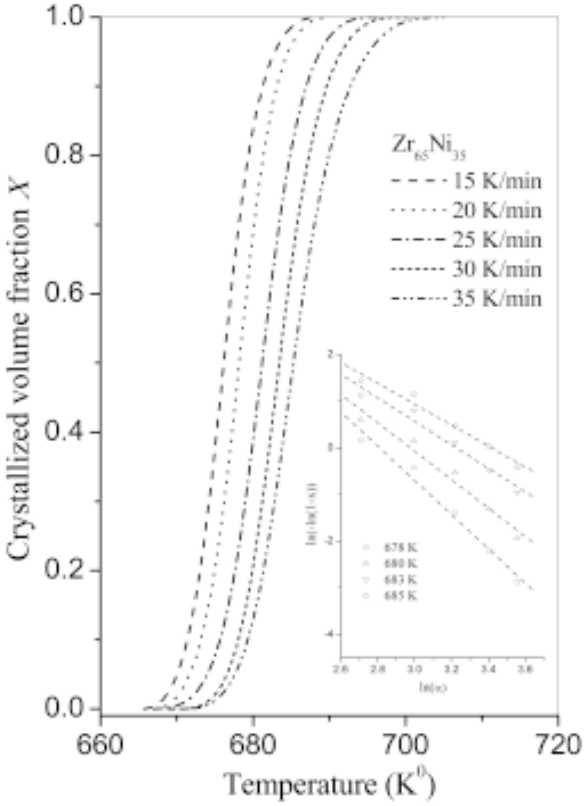

Fig. 4. The crystallized volume faction χ derived at different heating rates (15 – 35 K/min.) (see text). In the inset is the {ln(-ln(1-χ)) versus ln(α)} plot at constant temperature equation (3), where the Avrami exponents *n* can be derived from the slope of this plot.

smaller than those calculated for the FQ $Zr_{65}Ni_{35}$. Lee and Koch [11] observed similar results. Table 1 summarizes some of the thermal parameters derived for the FQ and MA specimens.

In order to understand the mechanism of the crystallization process in this system, an attempt is made to derive the Avrami exponent *n* which provides information about the nucleation and growth during the crystallization process. Therefore, Matusita formulation was used, which is based on the Johnson-Mehl-Avrami (JMA) equation, to describe non-isothermal DSC measurements as follows [12,13]

$$\ln(-\ln(1-\chi)) = const\ \tan t - n\ln(\alpha) - 1052\left(mE_a/RT\right), \quad (3)$$

where χ is the crystallized volume fraction, *n* is the Avrami exponent and *m* is the dimensionality of the growth which are both constants, having values between 1 to 4 depending on the morphology of the growth [14]. The crystallized volume fraction χ is derived from the first (main) peak for each alloy according to the procedure explained elsewhere [5] and is then plotted as a function of temperature at different heating rates. The relationship between volume fraction χ, heating rate α and temperature *T* for FQ $Zr_{65}Ni_{35}$ specimen, is shown in Fig. 4, where the well known S shape is clearly observed. A similar curve is obtained for the MA $Zr_{65}Ni_{35}$. It is possible to evaluate the Avrami exponent *n* from Eq. (3), by plotting ln[-ln(1-χ)] as a function of α, at constant temperature, where the slope gives n values. Such a plot is given as an inset in Fig. 4 and the *n* values obtained are summarized in Table 2 for both FQ and MA $Zr_{65}Ni_{35}$ specimens. The average value obtained for the Avrami exponent *n* is taken at four different temperatures and turns out to be 2.9 ± 0.3 and 2.8 ± 0.4 for the FQ and MA $Zr_{65}Ni_{35}$ specimens respectively. These values are in excellent agreement for the two specimens although the preparation methods are quite different, indicating that the thermal behaviour of the two amorphous specimens prepared by FQ and MA is almost similar under non-isothermal conditions. The computed *n* value is not an integer, suggesting that the crystallization process in the amorphous ZrNi system takes place through different mechanisms, where the predominant mechanism is close to $n \approx 3$ [15,16]. Since no prior heat treatment was given to nucleate the specimens before thermal measurements, the dimensionality of growth is taken to be equal (*n*-1) [13]. Therefore, the present results suggest that the crystallization process in present system proceeds in a two dimensional growth. Therefore, these results suggest that under non-isothermal conditions, the crystallization process in both the FQ and MA ZrNi is mainly dominated by a two dimensional growth.

4. CONCLUSIONS

FQ and MA ZrNi specimens were investigated under non-isothermal conditions. As a first step prior to the thermal studies, two FQ and MA $Zr_{65}Ni_{35}$ specimens were structurally compared using the radial distribution function *G*(*r*), in order to establish whether there are any structural differences on an atomic scale, and found to be structurally similar. The FQ $Zr_{65}Ni_{35}$ was found to be much more stable than its MA counterpart. The computed Avrami exponent *n* is about 3 for both specimens, suggesting that under non-isothermal conditions, the crystallization process in both FQ and MA ZrNi specimens is mainly dominated by growth in two dimensions. Moreover, these values are in excellent agreement for the two specimens although the preparation methods are quite different. This indicates that the thermal behaviour of the two amorphous specimens prepared by FQ and MA is similar under non-isothermal conditions.

ACKNOWLEDGEMENT

The FQ samples were prepared at the University of Sheffield, UK. I would like to thank Dr N. Cowlam, for providing facilities and J. Newell for help.

References

[1] C. Koch // *J. Non-Cryst. Solids* **117/118** (1990) 670.
[2] S. Chen, Y. Zhou and Y. Li // *J. Mater. Sci. Technol.* **13** (1997) 86.
[3] A. Al-Hajry, M. Al-Assiri and N. Cowlam // *J. Phys Chem Solids* **59** (1998) 1499.
[4] A. Al-Hajry // *Mater. Research Bulletin* **35** (2000) 1989.
[5] A. Soliman, S. Al-Heniti, A. Al-Hajry, M. Al-Assiri and G. Al-Barakati // *Therm. Acta* **413** (2004) 57.
[6] X. Wang, M. Qi and C. Dong // *J. Non-Cryst. Solids* **318** (2003) 142.
[7] B.S. Murty and K. Hono // *Mater. Sci. Engin. A* **312** (2001) 253.
[8] L. Liu and J. Zhang // *Mater Reasearch Bulletin* **36** (2001) 2073.

[9] B. Murty and S. Rangathan // *Int Mater Rev* **43** (1998) 10.
[10] H.E. Kissinger // *Anal. Chem.* **29** (1957) 1702.
[11] P.Y. Lee and C.C. Koch // *J. Mater. Sci.* **23** (1988) 2837.
[12] K. Matusita, T. Komatusa and R. Yokota // *J. Mater. Sci.* **19** (1984) 291.
[13] D.W. Handerson // *J. Non-Cryst. Solids* **30** (1979) 301.
[14] K. Matusita and S. Sakka // *Thermochim. Acta* **33** (1979) 351.
[15] J. Colemenero and J.M. Barandiaran // *J. Non-Cryst. Solids* **30** (1978) 263
[16] A. Morotta, S. Saiello and A. Buri // *J. Non-Cryst. Solids* **57** (1983) 473.